

# Atomic force microscopy using plastic replicas

J. B. CAMPBELL, J. LANKFORD  
Southwest Research Institute, San Antonio, Texas  
E-mail: [jcampbell@swri.org](mailto:jcampbell@swri.org)

Scanning probe microscopy is now an accepted tool in both industrial and research efforts. Its development parallels the advances in technology and imaging applications found in the history of progress of both transmission electron microscopy and scanning electron microscopy. All three forms of microscopy ultimately suffer a fundamental application problem—situations arise where it is either unreasonable or impossible to observe a particular sample within the sample stage of the microscope. For the transmission and electron and scanning electron microscopies, this problem has been resolved by resorting to making a replica of the area of interest on the actual sample and preparing the replica so that it may be imaged directly by the desired microscopy technique. This work attempts to ascertain the suitability of observing replicas using a scanned probe microscope; specifically, employing the techniques of atomic force microscopy to image plastic surface replicas. © 2000 Kluwer Academic Publishers

## 1. Introduction

Scanning probe microscopy (SPM), first introduced in 1981 through a demonstration of scanning tunneling microscopy [1], has advanced rapidly to the point of common use in industrial and research applications. The major advantages of SPM over conventional light or electron microscopy include atomic scale spatial resolution capabilities in both lateral and vertical dimensions, and the ability to attain high resolution without subjecting a specimen to either high vacuum conditions or bombardment with high energy particles, as in electron microscopy. Non-electrically conductive specimens or samples of a soft or delicate nature may be directly imaged. With appropriate fixturing, samples immersed in fluids may be imaged, and chemically reactive processes such as surface corrosion may be observed microscopically and recorded *in situ*.

However, scanned probe microscopy is not without certain disadvantages. The most common drawbacks encountered are probe tip artifacts, and the difficulty of actually mounting certain specimens for observation within the probe microscope. Probe tip artifacts generally fall into two categories of the same problem, whereby the scanned probe itself contributes some component of its own structure to the image. This may be in the form of convolution of the tip geometry into the imaged geometries of the features being scanned, or may be the result of the tip having single or multiple “sub-tips,” each of which contributes to the image. When scanning, the tip may pick up debris, which in turn act as pliant “sub tips,” that create noisy and unstable images. Fortunately, most of these problems are easily recognizable to the experienced microscopist, and may be corrected as simply (in the latter case) as replacing the tip. The problem of tip-to-surface geometry convolution can be more difficult to deal with. From

an operational standpoint, the probe microscopist must constantly compare the dimensions of the scanned features with assumed specific geometric dimensions of the applied tip, in order to objectively ascertain to what extent an image is an accurate representation of a surface.

The problems encountered in actually mounting a specimen for probe microscopy are usually determined by the nature of the experiment to which the microscopy will be applied. It has become increasingly desirable to use the probe microscope’s resolution capabilities to record and analyze time or cycle dependent data, as in friction and wear testing or in cyclic fatigue studies of materials. These types of experiments require a viable specimen for an extended period of time; the basic experiment consists of observing the response of a discrete area over that period of time or cycle space. Thus, sectioning of a specimen to fit within a probe microscope would prematurely terminate the experiment.

In these types of experiments, the specimen must be of a size large enough to be correlatable to the real-world phenomenon that the experiment has been designed to investigate. They must also be of sufficient size and proper construction to be installed in the testing apparatus in which the experiment is to be performed. Scanned probe microscopes have been constructed in which large samples may be observed, or that involve observation by means of literally placing the microscope itself onto the large object to be imaged. However, in the materials engineering field, most specimens are usually of complex geometry, such that they are impossible to fit within even a nominally large-sample probe microscope.

The problem of observing a sample microscopically without destroying it is not a new one. The problem of observability is further compounded if it is found to be

necessary to examine a specimen in a state of physical loading; for example, an observation of a fatigue microcrack held at its maximum stress state. This would require that the microscope be attached to the specimen loading apparatus, or that the entire loading apparatus and specimen be miniaturized and fitted within an SEM chamber for observations at superior resolution to be made under load. The latter has been achieved [2], and recently a miniature loading apparatus has been devised to operate within the stage of a scanned probe microscope [3]. However, both SEM and SPM loading stages accommodate only highly specialized specimens, and though the SEM loading stage has more flexibility in terms of the specimens it will accept, the SEM loading stage does not offer the resolution capability of the probe microscope. It is evident that most situations occur in which the only possible method of examining a discrete area on a sample with SPM is by microsectioning the sample, and thus destroying it.

Fortunately, the techniques of surface replication are available, and have been effectively employed to examine samples nondestructively by light, scanning, and transmission electron microscopy [4]. Replicas can easily be made of samples held under load in testing machines. It is therefore reasonable to hope to be able to apply SPM, specifically Atomic Force Microscopy (AFM), to the examination of surface replicas of sample materials.

However, the extraordinary resolution capability inherent in AFM, and the operating principles involved in its imaging process, necessitated a systematic investigation of the validity of its application to surface replication techniques. In the following, resolution limits of the technique are investigated, and the role of tip geometry is examined; this is found to have significant effects on resolution. Correlative microscopy using AFM and SEM is performed on the same area of a specimen and on replicas of that area. TEM replicas of the area are also examined for comparison. Ultimately, the work examines the accuracy of the replication process itself.

## 2. Procedures

A material of sufficiently fine microstructure was necessary to produce a good test of the limits of resolution made available with the replication technique. It also was desirable that the material possess a microstructure of easily recognizable and repeatable features. The intermetallic  $\gamma$  titanium aluminum, with which the authors have had considerable experience [5], was found to meet these criterion. The microstructure consists of large colonies of close-packed, unidirectional lamellae of about  $1.2\ \mu\text{m}$  average size. Stoichiometrically, the lamellae are randomly alternating sheets of  $\text{Ti}_3\text{Al}$  and  $\text{TiAl}$  phases that solidified from the melt solution in varying crystallographic orientations. The lamellae can be of exceedingly fine thickness; lamellae thicknesses of  $150\ \text{nm}$  are common.

A small block of material was metallographically polished to a  $0.05\ \mu\text{m}$  finish, and then ion etched under a  $6\ \text{KeV}$  nitrogen beam generated by a duoplasmatron source, using a beam incidence of  $30^\circ$  to the specimen

surface. The etching process was performed in increments of 15 minutes under the same conditions, with microscopic examination of the specimen at the finish of each increment, to avoid overetching of the specimen. Two etching increments for a total of 30 minutes of ion etching were used to produce a low topography, high frequency surface of less than  $100\ \text{nm}$  height differentials. Additionally, a freshly cleaved mica surface was replicated and the replica examined by AFM as a means of testing the replica's response in the ultrastructural size range.

In order to perform true correlative microscopy, a knoop hardness indentation was used to mark a selected area of microstructure (near the tip of the indent) for repeatable exercise of the several microscopy techniques. SEM examinations were performed with a Philips XL-40 equipped with a  $\text{La B}_6$  cathode; under optimum condition, this microscope is capable of  $3\ \text{nm}$  resolution. Initially, a Digital Instruments Nanoscope II<sup>®</sup> was used to perform AFM characterization in ambient air, using contact-mode techniques. Subsequently, a Digital Instruments Nanoscope III was used to examine a similar microstructural area and its replica. Tapping mode imaging was used in that experiment. AFM imaging in tapping mode eliminates the shear forces developed in contact mode imaging, enhancing AFM's resolution and providing a more artifact-free image by limiting the AFM tips mechanical interaction with the scanned specimen. This provides major advantages when scanning compliant or delicate surfaces, or, as will be seen, surfaces with fragile, atomically-thin coatings. A Philips EM 420 TEM was used to study the replicas in electron transmission. Multiple replicas of the indent tip were prepared and imaged by the AFM to gauge the repeatability of the replication and imaging process.

For this work, several thicknesses of replica material were used to test thickness effects on resolution; no dependence was found. All work reported here was from replicas made from cellulose acetate film of  $35\ \mu\text{m}$  thickness.

Replication procedures were the same for AFM and SEM examination. The specimen to be replicated is wetted with acetone, a solvent of the replicating material. Using forceps, a film of replicating material is then brought into contact with the wetted specimen; the replicating material is then either left undisturbed until the solvent has completely dried, or finger or clamping pressure is applied to the replica back using a soft material such as a rubber compound as an intermediate medium between the finger or the clamp. Once the replica is thoroughly dried, double-sided tape is cut to proper size and gently pressed onto the back of the replica. This tape-replica assembly is then lifted from the specimen and mounted by inverting the assembly and attaching it to the appropriate microscope stub holder by using the exposed double-sided tape surface. Care must be taken to make the replica-tape assembly as flat and as parallel to the stub surface as possible, to achieve maximum lateral AFM scans.

For SEM observation, the replica must be coated with a conductive film to dissipate electrical charge and to

protect the replica from damage induced by the electron beam. Though AFM imaging does not require conductive coating, other practical considerations require some thin film coating to be applied to the replica for AFM imaging. The primary consideration is to make the replica optically reflective so that a discrete area of interest may be placed under the AFM tip by use of the optical positioning microscope. When using contacting mode AFM, the AFM tip touches or resides very close to ( $>2$  nm) the replica surface; a coating thus helps protect the replica from tip damage. This effect is not so significant when scanning with a large radius,  $136^\circ$  pyramidal  $\text{Si}_3\text{N}_4$  tip. However, contact-mode scanning performed with the high aspect ratio single crystal silicon tips can severely damage a plastic replica, even when scanned under the least practical force available. On the other hand, high aspect ratio tips offer superior resolution and increased freedom from tip shape artifacts. High aspect ratio tips were used in the tapping-mode imaging studies.

Clearly, the microstructure of the coating itself must be of a sufficiently fine scale to escape detection by the AFM. The coating also should be thin with respect to the fine scale vertical topography to be imaged; if it is too thick, it will compress or even completely cover vertical height differentials. For this work, sputtered tungsten coatings were adjusted to a final thickness of about 3 nm, which provided suitable conductivity and reflectivity for SEM and optical examination and sufficient quality for protection from the scan forces induced by the  $136^\circ$   $\text{Si}_3\text{N}_4$  tip, but were marginally adequate for AFM examination with high aspect ratio silicon tips. All coatings were applied with a VCR IBS-200 sputter coater.

Replicas for transmission electron microscopy (TEM) examination were prepared using standard techniques. In this case, plastic replicas were applied using acetone as a solvent, stripped off, and, using a vacuum coater, shadowed with palladium followed by coating with carbon. The plastic film was dissolved using acetone, and the resulting metal-carbon replica was applied to a standard TEM specimen grid. The foils were then examined using the 200 KeV Philips 420 TEM.

### 3. Results

AFM replicas of the freshly cleaved mica sample showed no discernable atomic structure when imaged in any of the AFM scan model/tip combinations available. The images did present a “webbed” texture. This texture was apparent in comparable scans taken from replicas of the metallic sample. This phenomenon may be an intrinsic replica “background noise.”

Multiple replicas of the indent tip as imaged by the AFM displayed little detectable variability between images, suggesting good repeatability of technique. Shown in Fig. 1 is an SEM image of the TiAl microstructure near one end (arrow) of a reference indentation in an actual specimen. Plate-like microstructural elements appear to be serrated, due to the presence of elongated subelements. For reference purpose “A” and “B” denote two short “platelets” nearly in line with one

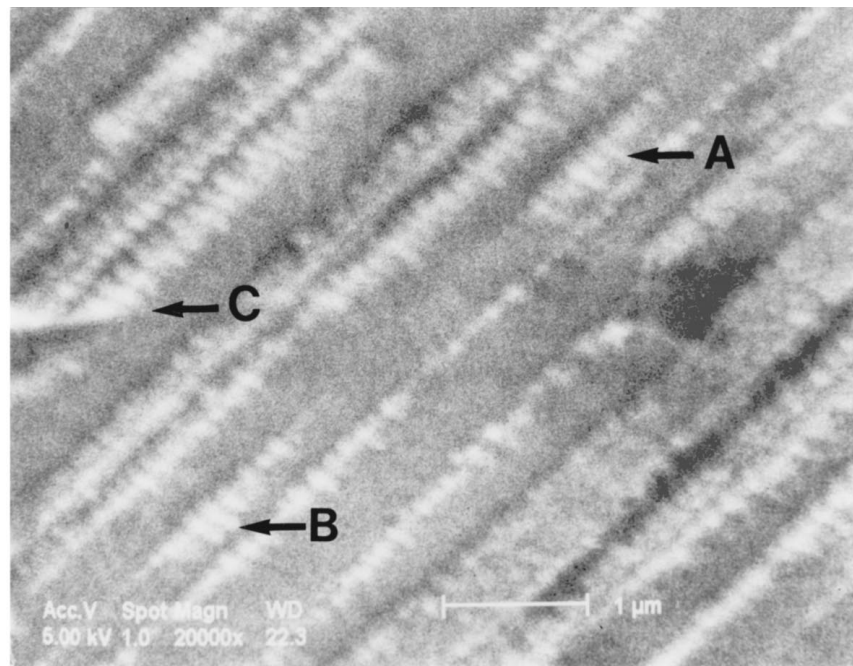
another; it will be convenient to use these as references in comparing images obtained by other means.

Thus, the same region is shown in Figs 1b and 2 at the same nominal magnification (20,000X) by SEM and TEM of surface replicas. The SEM version of the replica (Fig. 1b) seems remarkably true to that of the actual surface (Fig. 1a), while the transmission microscope version looks somewhat different. In the latter case, the discrete nature of the platelets is diminished, but at the same time, the elongated subelements appear to be exaggerated. Microstructural subelements within the carbon coating of the TEM replica may be responsible for the fine scale collateral background contrast, or the contrast may be the result of the above-mentioned replica “background noise.”

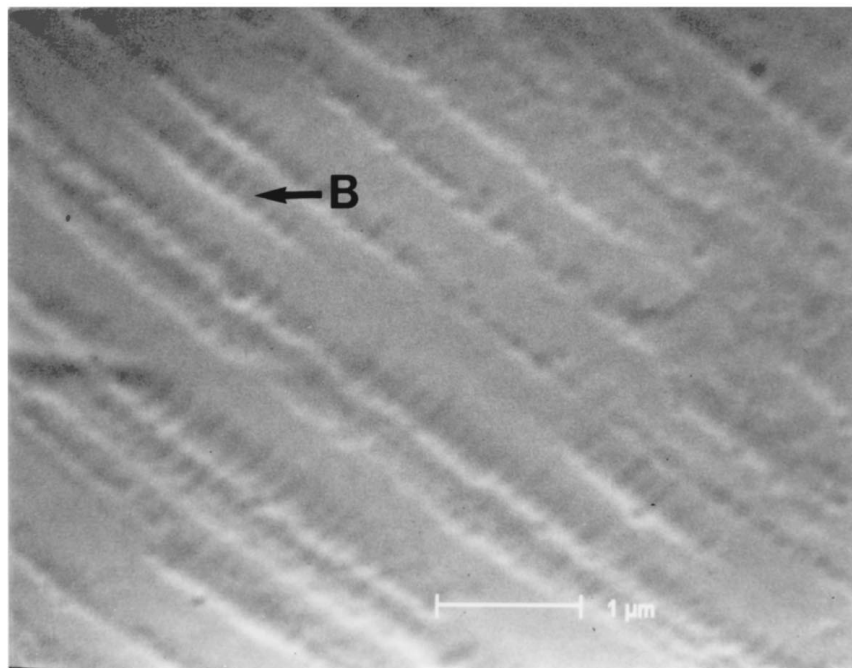
Atomic force images of the sample surface generated using  $136^\circ$  pyramidal tips (Fig. 3a) provide much greater detail than that seen in the SEM (Fig. 1). However, the same tips operating on replicas yield diffuse images lacking in detail (Fig. 3b). The observation of the loss of comparable resolution between replica and surface images led to an investigation of the effect of tip geometry and the mode of imaging on the AFM’s ability to resolve this surface. The initial replica imaging was performed using  $136^\circ$  tips in contact-mode; it was postulated that the high-aspect ratio tips employed in contact—or tapping-mode could improve resolution by providing a probe of finer geometry. Additionally, tapping-mode should alleviate micro-compliance (surface-movement) effects which could hamper or confound resolution. Image quality is, in fact, significantly enhanced for both sample and replica by employing the high aspect ratio Si tip, as shown in Fig. 4a and b. The details associated with elongated subelements is particularly clear.

Even though the replica was lightly coated with tungsten, sharp tip artifacts (streaking) were introduced with repeated scans in the contact-mode. These did not occur on repeat scans of the sample itself using the sharp AFM tip, nor did they occur when imaging the replica in tapping-mode, with the high aspect ratio tip. Fig. 5 shows an indent tip imaged by tapping-mode using a high aspect ratio tip. The actual surface and replica of the same area are compared, and though the areas appear to be quite similar, a definite breakdown of correlation between the images is apparent. The diffusion of resolution is profound at higher magnifications, as illustrated in Fig. 6. Again, a replica image and an image of the actual surface taken of the same region are compared.

The effect of the diffusion of resolution between sample and replica was revealed by obtaining AFM profiles of equivalent traces along samples/replica surfaces. This is shown in Fig. 7, where it can be seen that although the profiles are similar in shape, that corresponding to the (positive image) replica is significantly “flattened,” compared to the sample. Analysis of nominally equivalent locations along these profiles indicates that the average amplitude of a replica point relative to a neutral horizontal centroid is on average 64% of the actual sample height (no significance should be construed in the lack of correlation in fine scale detail in



(a)



(b)

Figure 1 (a) SEM micrograph of surface of  $\gamma$ TiAl specimen with edge of knoop hardness indent at left of photo field, C. A and B are short platelets referenced for comparison in succeeding figures. (b) SEM image of replica taken from area in (a).

the two traces, since clearly the AFM tip cannot follow precisely the same path along two physically distinct specimens). Furthermore, analysis of  $x$  and  $y$  dimensions of the same feature between replica image and actual sample surface images show a divergence in lateral dimensions from the dimensions measured on the actual surface.

#### 4. Discussion

It appears that atomic force microscopy of plastic surface replicas can provide an excellent means of

monitoring and characterizing nanoscale changes in material ultrastructure, down to a limiting scan size range. However, standard pyramidal AFM tips, at least when operating in the scanning force mode, provide somewhat less resolution of replica details. Sharp, high aspect ratio tips provide better resolution of detail, although when employed in contact-mode, they quickly degrade the replica surface, with attendant loss of image quality and the production of artifacts. This was not the case when the high aspect ratio tips were used in tapping-mode imaging. Shear forces developed during imaging in contact-mode are greater for the high

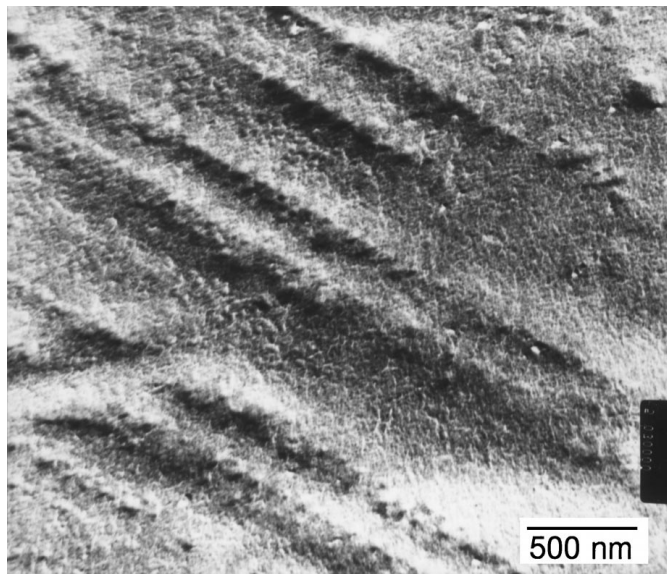
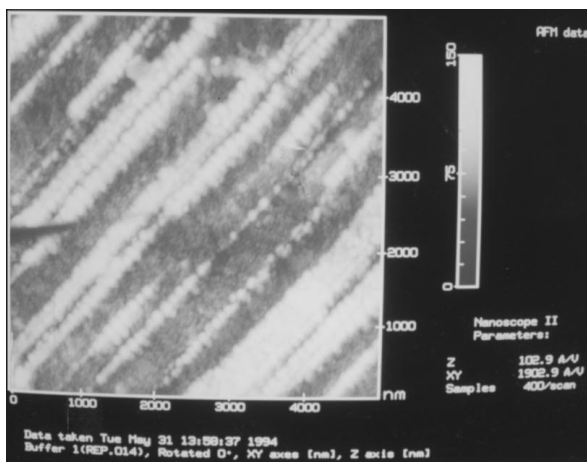
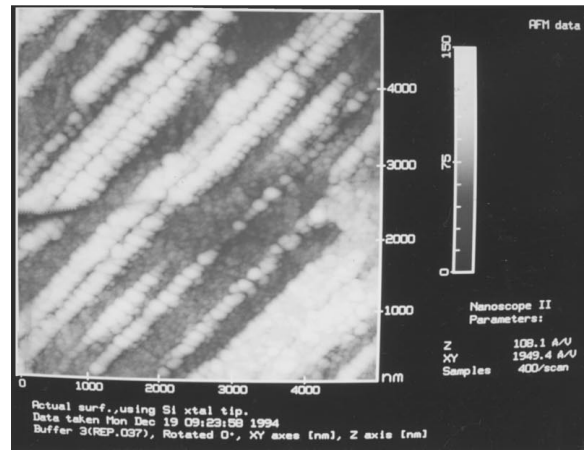


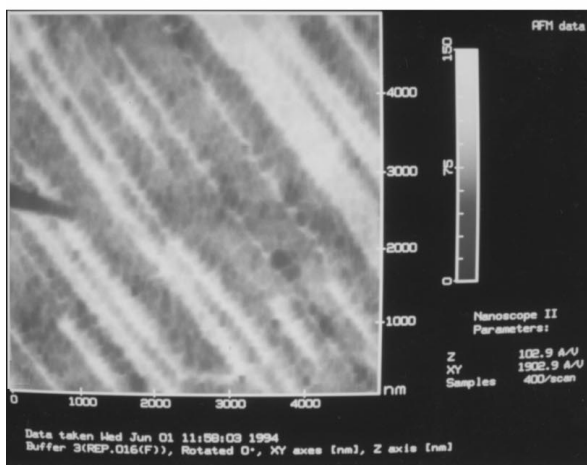
Figure 2 TEM image of replica taken from area in Fig. 1a. Finer detail is apparent between major features, but it is unclear if the detail is artifact from the replication processes or is actually real detail present on the  $\gamma$ TiAl surface.



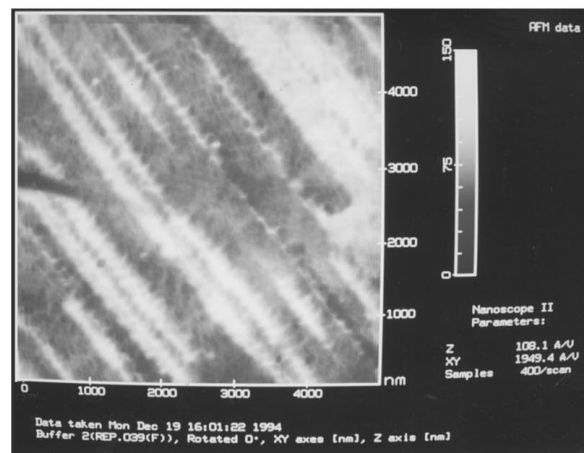
(a)



(a)



(b)



(b)

Figure 3 (a) AFM image taken with  $136^\circ$  pyramidal tip of area in Fig. 1a. Much greater detail is apparent. (b) AFM image of replica taken in area in Fig. 1a. The image is displayed in inverted format, as are all subsequent AFM replica images, to enable the viewer a closer correspondence in comparing the images. The replica image, though true to the actual surface in a macroscopic sense, has lost much detail, and fidelity to the image of the actual surface.

Figure 4 (a)  $\gamma$ TiAl surface in the area of Fig. 1a imaged with high aspect ratio single crystal Si tip in contact-mode. Resolution seems to be improved; balled lamellae (the raised features running diagonally across the image, roughly ball-shaped) lines seem broader than when imaged with the  $136^\circ$  pyramidal tip. (b) Replica of Fig. 1a area imaged with high aspect ratio tip; macroscopic features and orientations are faithful to the image of the actual surface and the resolution seems better than that in Fig. 3b. However, at finer scale, the fidelity diverges from the parent image, Fig. 4a.

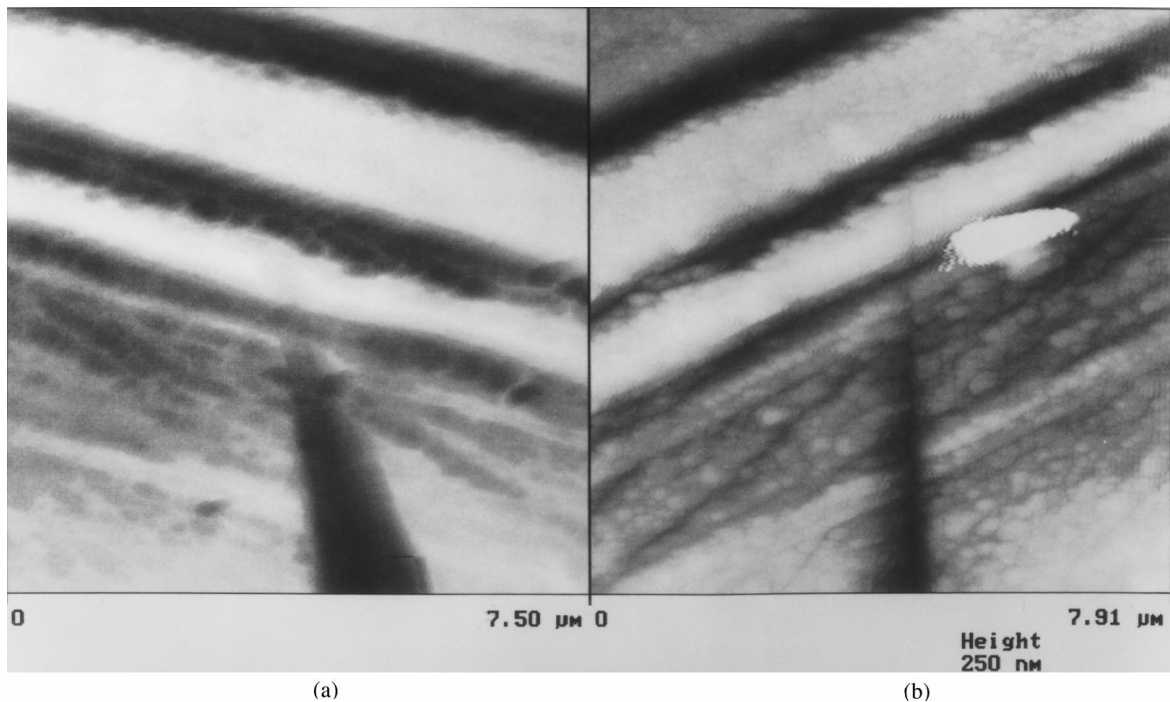
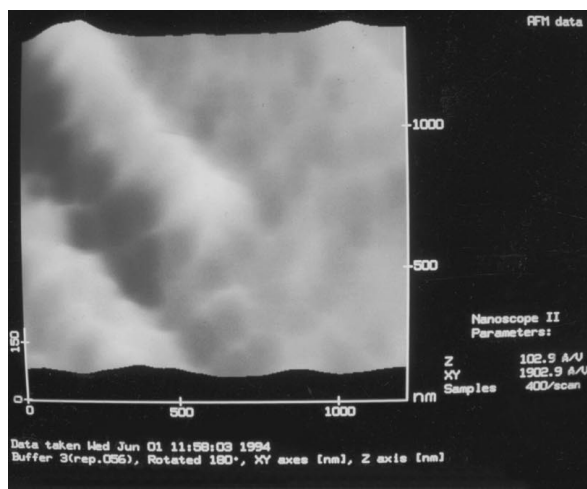
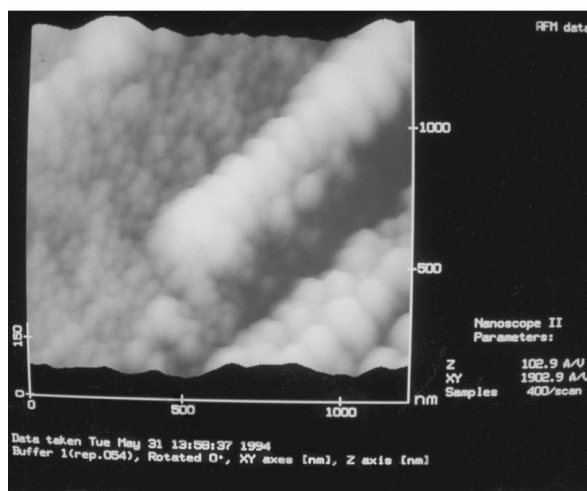


Figure 5 (a) Replica image of actual surface area about a knoop hardness indent in a similar specimen of  $\gamma$ TiAl. (b) Actual surface. These images were taken by AFM in tapping-mode using Si high aspect ratio tips. Again, the divergence of fidelity displayed by the replica is evident.



(a)



(b)

Figure 6 (a) Replica image and (b) actual surface image of same area on  $\gamma$ TiAl specimen. Images were taken with the same  $136^\circ$  pyramidal tip in contact-mode. The loss of fidelity/resolution by the replica becomes very apparent at smaller scan sizes.

aspect ratio tips than for the  $136^\circ$  pyramidal tips; the higher shear forces are probably stripping the tungsten coating from the replicas, thus producing the observed artifacts. Regardless, replicas scanned by AFM have higher resolution capability than an equivalent SEM image, and offer the advantage of providing easily accessible quantitative vertical height information, and AFM images suffer no foreshortening effects induced by the tilting often required for high resolution SEM or TEM imaging.

Most important was the observation that the image resolution and average topographic replica feature measured by the AFM was significantly reduced in Z-amplitude and distorted in lateral dimensions versus that measured on the actual sample. This degradation of replica accuracy was slightly less for tapping-mode imaging with high aspect ratio tips, but is profound and similar regardless of tip or imaging mode. Qualitatively, the replica images appear to hold much less detail than the true surface images. Anecdotaly, the major features in the replica images have the appearance of being draped or covered in a manner analogous to a room full of furniture being covered by painter's drop cloths. Upon close examination, the "draps" of the replica images are made up of curved facets linked by extruded creases, giving the impression of a webbed texture. The texturing seems to indicate a fine scale replica collapse, i.e., the replicating material dried or pulled away before the surface impression was fully cast in the material. This phenomenon is common and has been observed on a much larger, but still microscopic, scale in both TEM and SEM replicas [6]. As previously stated, a similar webbed texture was observed on replicas taken from atomically-flat, freshly-cleaved mica surfaces, and is apparently a contributing mechanism in the replica's loss of resolution/loss of fidelity. Fig. 8 is a plot of the dimensional divergence in X, Y, and Z of the features measured on AFM replica images from the same

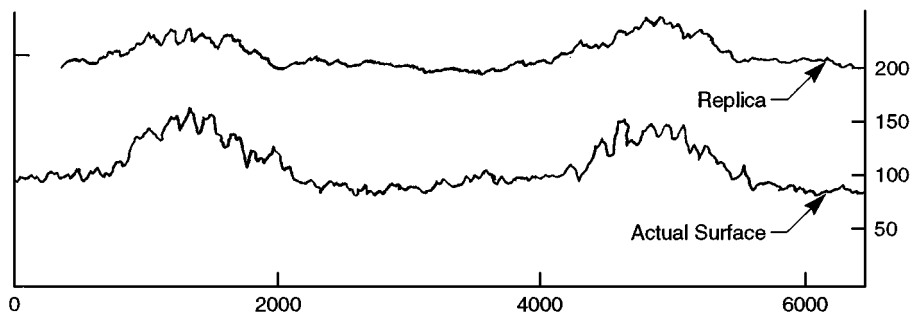


Figure 7 A cross section profile, taken down the center lines of features A and B in Fig. 1a, from AFM images of the actual specimen surface and a replica of the same area. The replica cross section trace is presented non-inverted and rotated such that it should appear in an “as lifted” orientation over the features of A and B on the  $\gamma$ TiAl surface. In this comparison, it becomes evident that larger scale vertical and lateral correlation between the images is reduced, as well as a loss of fine scale detail content. The reduction of vertical fidelity appears to be on average about 64%.

### x,y, and z divergence, measured feature

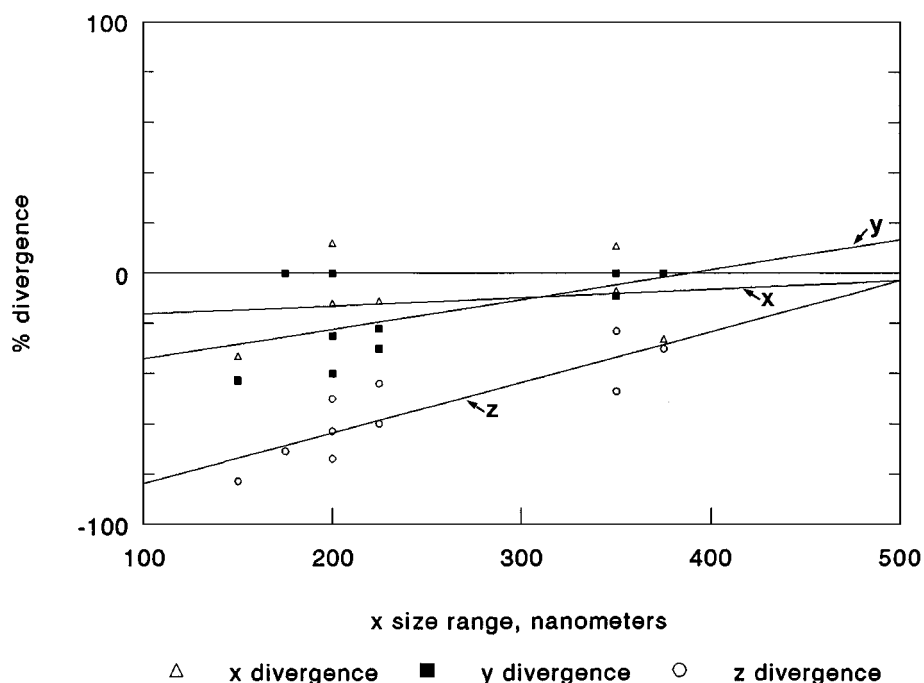


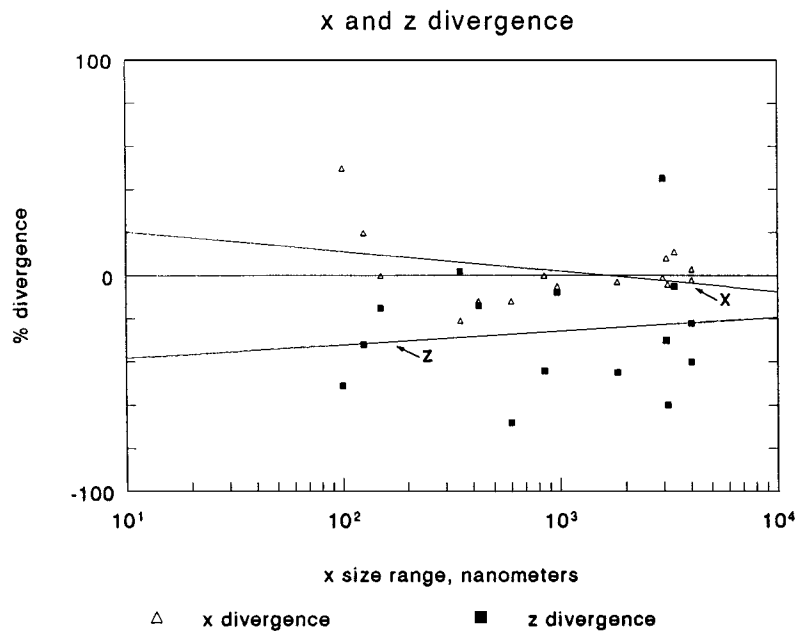
Figure 8 Replica dimensional divergence from the surface over which it was cast. The same surface features were measured in AFM images of the actual sample surface and on replicas of the surface. The measurements are  $x$  and  $y$  cross sections of the features, taken as closely as possible in the same position relative to the feature. The  $Z$  (vertical) dimensional measurements were performed in the same manner. The  $x$  (lateral) size of the features was arbitrarily selected as the ordinate ( $X$ -axis). Percent divergence is the percent difference of the replica measurement from the measurements made on the real surface.

features measured from AFM images of the actual sample surface, with the  $X$ -axis being the  $X$ -dimension of the feature as measured on the real sample surface.  $X$ ,  $Y$ , and  $Z$  measurements were taken by the Nanoscope II cross section software. The measurements were taken as closely as possible along the same profiles of the features between real surface and replica image. Measurements  $x$  and  $y$  were performed co-axially to the  $x$  and  $y$  microscope scan directions, respectively, to reduce error as much as possible.

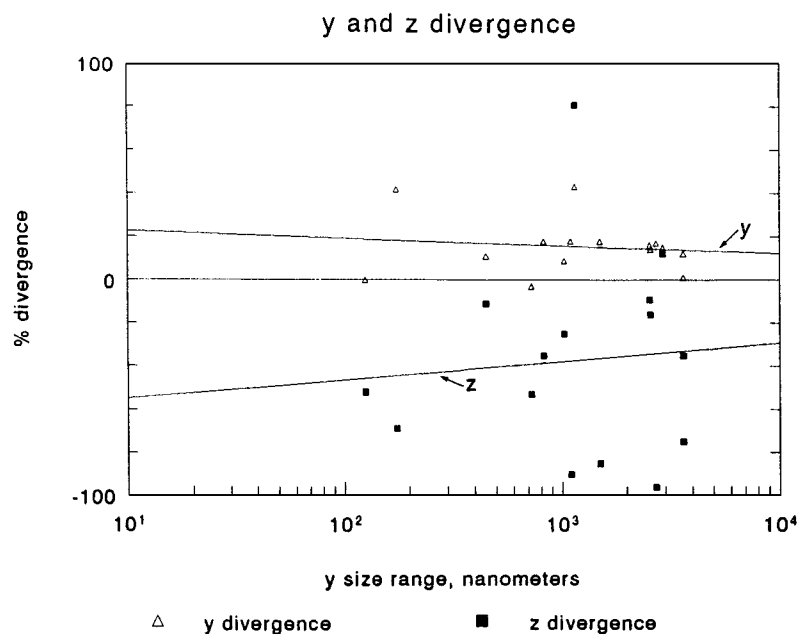
Quantitatively, the plot shows a marked, negative divergence from the measurements of the same features, as seen on the real sample surface, with the vertical measurements displaying greater divergence than that apparent in the lateral dimensions. The divergences increase as the size of the measured feature decreases.

A similar graph comparing profile line cuts in  $x$  and  $y$  scan directions along the same paths on both replica and real surface images is shown in Fig. 9. Again, the plot is the replica's divergence from the real surface measurements, dependent on the  $x$  or  $y$  dimension as measured on the real surface. It shows similar behavior to the first plot: a marked negative divergence with decreasing feature size that is quite pronounced for the vertical measurements. Interestingly, the  $Y$ -scan replica measurements tend to diverge to the positive. Both plots show good lateral dimension correlation between the true surface and the replica surface above an  $x$  or  $y$  scale of about  $4 \mu\text{m}$ ; vertical dimensional correlation, however, remains poor.

Many factors probably are working to create the differences in measured dimensions observed between the



(a)



(b)

Figure 9 Replica dimensional divergence from the actual surface as measured using cross section profiles in  $x$  and  $y$  scan directions. Cross section profiles were taken as in Fig. 7, and feature spacings and relative vertical dimensions were compared. Measurements were performed by selecting easily recognizable sets of maxima or minima along the section profiles taken across the same segment of surface and replica image. The  $x$  or  $y$  spacings and their relative vertical differentials were then recorded. As in Fig. 8, percent divergence is the percent difference of the measurements made from the replica image from the measurements of the same points made from the actual sample surface. (a) Data plotted from  $x$  cross section measurements, with the ordinate as the  $x$  size as measured on the actual surface. (b) Data plotted in the same manner for  $y$  cross section measurements.

real and replica surfaces. Much detail is lacking in the replica images versus those of the true surfaces. This ensures that selecting the same sections for measurement on the replica as on the real surface image is a difficult and necessarily subjective task.

The  $\text{Si}_3\text{N}_4$  pyramidal tips probably do not accurately trace the smaller depressions left by features over which the replica was cast. This is due to the fact that the tip never goes to the bottom of depression, due to its relatively large radius, and its low aspect ratio makes it

quite probable that the pyramid's sides interact with the edge of the depressions, introducing side or face artifacts and further limiting the amplitude of penetration of the tip. One would not expect to see this effect on vertical features of large spacing ( $>1\ \mu\text{m}$ ), yet the  $Z$  divergence is clearly apparent and much larger than the lateral divergence in the low frequency component of Fig. 6 and on the line cuts of Fig. 8. This tends to indicate some problem intrinsic to the replication process. A possibility is shrinkage of the acetate leading to



subsequent premature detachment, drying and resultant loss of dimensional reproduction (and possibly attendant poor detail resolution).

In consequence, this would suggest that any observations based on replica imaging (AFM, SEM, or TEM) may be suspect. Such errors might not be apparent via normal imaging, since the essential details would be present (but distorted in terms of height aspect ratio). Only nanoscale profilometry would be capable of resolving the effect (as here), which may be (and have been) present but undetected in the SEM observations of numerous other investigators. Height information derived from surface replication therefore should be verified, and not accepted at face value; similarly, fine-scale details associated with rapidly-changing topography may be distorted, and should be suspect. Accepted resolution limits for replicas are approximately 5 nm for direct carbon replicas and 10 nm for plastic-carbon replicas, when examined by TEM [7]. The smallest ultrastructure observed on the  $\gamma$ TiAl sample is on the order of 8–10 nm. Some of the finer creases in the webbed texture observed on the replica images measure about 10 nm in width. However, these features clearly do not accurately represent the actual microstructure over which they were cast. Thus, the resolution limit of the AFM when applied to replicas is defined by the fidelity of the replica itself, rather than by the resolving ability of the AFM. For the material prepared and replicated in this work, the resolution limit appears to be about 250 nm.

## 5. Conclusions

It is not surprising that an instrument capable of atomic scale resolution that is discretely derived from the absolute surface of the sample to which it is applied should reveal artifacts and fidelity errors associated with the techniques of surface replication. Nonetheless, AFM of replicas offers higher resolution than that obtainable

from replicas imaged by conventional (non-field emission) SEM. TEM-scale resolution is available by AFM replica technique in a fraction of the time necessary for the preparation of TEM replicas. Direct measurement of vertical and lateral dimensions, and their angular relationships, are quickly available, and the AFM images are free of electron optical and interaction artifacts. However, it is apparent that any dimensional measurement, taken below some critical scan size on a replica, has a large probability of being inaccurate. The divergence data developed in this work can be used as a general guideline as to the replica error one can expect to encounter for a given scan size on a replica taken from a flat, relatively very smooth surface. If one is contemplating using an AFM to gather data from replicas, one should first, as a calibration of technique, repeat, to some extent, the correlative work done here for the material, desired resolution, and surface morphology that one expects to encounter in actual experimentation.

It is clear that the replica is not a perfect "negative" copy of the surface from which it was taken. Accordingly, superior replication technology must be developed if replicas are to be useful in work that requires the AFM to be used in its higher resolution modes.

## References

1. G. BINNIG and H. ROHRER, *Helv. Phys. Acta.* **55** (1982) 726.
2. D. L. DAVIDSON and A. NAGY, *J. Phys. E., Sci. Instruments* **11** (1978) 207–210.
3. M. GÖKEN, H. VENHOFF and P. NEUMANN, *Scripta Met.* **33** (1995) 1187–1192.
4. *Metals Handbook*, Vol. 9, 8th ed., (1974) pp. 24–25, 63–64.
5. D. L. DAVIDSON and J. B. CAMPBELL, *Met. Trans. A* **24A** (1993) 1555–1574.
6. *Metals Handbook*, Vol. 9, 8th ed. (1974) pp. 281–296.
7. *Metals Handbook*, Vol. 9, 8th ed. (1974) p. 55.

*Received December 1996  
and accepted September 1997*